Mechanical and Aerospace Engineering
B. Guan (Ed.)

doi:10.3233/ATDE250020

Effect of Key Design Parameters on the Aerodynamic Performance of the Circulation Control Airfoils

Yanjun HOU [a,b,c,d1] , Ziang GAO [a] , Yi LIU [a] and Jian ZHANG [a]
[a] *Institute of Engineering Thermophysics, Chinese Academy of Sciences, Beijing, 100190, China*
[b] *School of Aeronautics and Astronautics, University of Chinese Academy of Sciences, Beijing, 100049, China*
[c] *National Key Laboratory of Science and Technology on Advanced Light-Duty Gas-Turbine, Beijing, 100049, China*
[d] *Key Laboratory of UAV Emergency, Rescue Technology, Ministry of Emergency Management, Beijing, 102202, China*
ORCiD ID: Yanjun Hou https://orcid.org/0009-0009-2301-6201

Abstract. Circulation Control (CC) is widely researched because it can generate high lift and create the effect of 'virtual control surfaces'. Currently, the relationship between the design parameters and the control effects of circulation control is not yet clear. Therefore, this paper establishes the airfoil parametrization method for circulation control airfoils and the effects of different nozzle heights, radii and shapes of Coanda surface, and airfoil thickness and camber on circulation control effect are investigated. The results show that the best equivalent lift-to-drag ratio (K_E) is at a nozzle height of $h/c = 0.06\%$; K_E peak at a Coanda surface radius of $a/c = 0.016$ and stabilize thereafter; the optimal Coanda surface shape is at $b/a = 3/2$. Increasing airfoil thickness and camber improves pitch moment but reduces K_E. The best overall performance is achieved at $t/c = 15\%$ and $w/c = 0\%$.

Keywords. Circulation Control, Airfoil parameterization, equivalent lift-to-drag ratio, Aerodynamic Performance

1. Introduction

The aviation field is continuously evolving in the 21st century, and modern warfare is increasingly becoming more intelligent and efficient. For future aircraft, ultra-short takeoff and landing, maneuverability, and high stealth performance have become key performance indicators [1]. The drawbacks of mechanical control surfaces are gradually being exposed. The gaps and movement of the control surfaces can disrupt the smooth geometric shape of the fuselage, thereby increasing the scattering area of the fuselage. Mechanical control surfaces can experience vortex breakdown during large-angle deflection, posing safety hazards. Therefore, there is a need to find a new control method.

[1] Corresponding Author: Ziang Gao, gaoziang@iet.cn.

Circulation control (CC), as an active flow control method, has been shown in studies to generate aerodynamic 'virtual control surfaces' [2]. The main principle behind CC is the Coanda Effect. When CC is applied to the convex surface at the trailing edge of a wing, a tangential jet is expelled from one side of the convex surface. As long as the pressure difference between the surface and the ambient air is equal to the centrifugal force generated by the deflection of the airflow, the jet will adhere to the convex surface and flow along it. CC delays boundary layer separation, changes the position of the stagnation point, increases the circulation around the airfoil, and thereby significantly enhances the lift of the airfoil [3]. The surface to which the jet adheres is known as the Coanda Surface. An airfoil with a Coanda surface is referred to as a Circulation Control Wing (CCW).

Englar conducted research on the effectiveness of early CC technology, focusing mainly on its high lift and short takeoff and landing performance [4]. Englar's pioneering work also showed that there is a nonlinear relationship between the increase in lift coefficient C_L and the blowing momentum coefficient C_μ, characterized by a boundary layer state at low blowing and a transition to CC state when the blowing C_μ reaches a certain value. At the beginning of the 21st century, Clyde and his team realized that CC was not a means of generating high lift, but a means of providing control forces [5]. This is because the demand for bleed air to generate useful control forces is only 1-2% of the engine exhaust. DEMON, which had its first flight in 2010, achieved roll control entirely relying on circulation control [6]. In 2019, MAGMA achieved the full replacement of conventional flight control mechanisms with active flow control. Luo's team integrated synthetic dual jets, proving the three-axis control capability of dual jets [7].

CC is an efficient control technology for aircraft, with research directions mainly focused on Coanda surfaces, jet expulsion methods, and control effects. However, the relationship between the shape design parameters and aerodynamic characteristics of CCW is still unclear. Therefore, this study aims to explore the effects of key design parameters of the circulaton control airfoil on its aerodynamic performance, laying the foundation for subsequent airfoil optimization efforts.

2. Physical and Numerical Models

2.1. Numerical Computation Methods

When validating the computational cases of circulation control airfoils with jet, the CC020-010EJ airfoil [8] is selected. The reference chord length of the airfoil is $c = 8.6in$, and the far-field boundary is 25 times the reference chord length. The height of the first layer of the grid ensures that the wall function measurement value y^+ remains within the range of (0,1). Figure 1 shows the structured grid. The far-field conditions are set as $Ma = 0.1$, $Re = 5 \times 10^5$, and an attack angle of 0 degrees.

Under the same conditions as [8], the SA turbulence model and the k-Ω SST model are applied respectively. The far-field velocity inlet and pressure outlet are set. The compressor cylinder inlet is set as a pressure inlet. From the perspective of the lift-to-drag ratio, the SA turbulence model provides a better fit. While the SA turbulence model fits better at the trailing edge Coanda surface. This study focuses on the impact of CC jet flow. Therefore, the SA turbulence model is selected for this study.

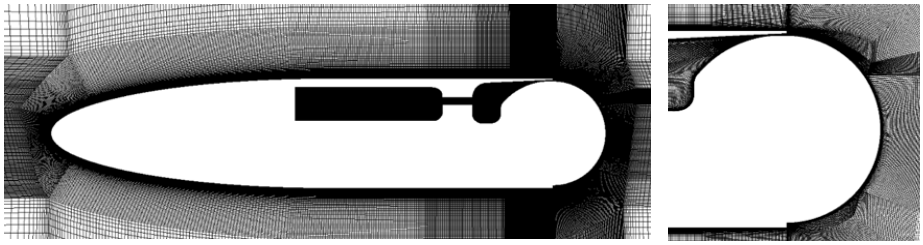

(a) Airfoil **(b)** Coanda Surface

Figure 1. CC020-010EJ airfoil structured mesh.

2.2. Airfoil Parameterisation Methods

The commonly used airfoil parametrization methods can generally be divided into two categories. One is the method that strictly defines the airfoil expression based on the geometric characteristics of the airfoil, such as the NACA airfoil [9] and GA(W) airfoil. The other is the highly adaptable linear fitting parametric expression methods, such as the CST method and the NURBS method.

This study focuses on airfoil geometric characteristics. So the basic airfoil refers to the parametric method of the NACA airfoil. Changes in the Coanda surface will cause changes in the height of the airfoil's trailing edge, thus introducing the trailing edge thickening method, as shown in equation (1). When simplifying the design of the wing jet, the effects of the compressor cylinder and nozzle wall thickness are not considered. The NACA four-digit airfoil are defined by mathematical expressions. The geometry of the Coanda surface is defined by several characteristic parameters. The main features of the basic airfoil include: maximum thickness t_{max} and maximum camber h_{max} of the mid-arc. The main parameters of the Coanda trailing surface include: nozzle height h, longitudinal a and transverse b axes of the Coanda surface. The airfoil parameter description is shown in Figure 2 below.

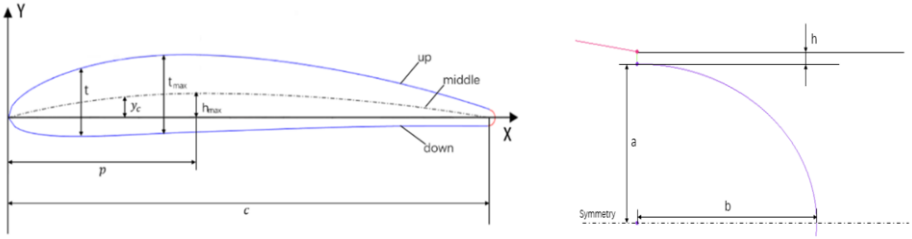

(a) Foundation Airfoil **(b)** Coanda Surface

Figure 2. Schematic diagram of relevant geometric parameters of airfoil.

The expression for the airfoil thickness is:

$$t_e = 2(a + h) \tag{1}$$

$$t = t_F + t_e \frac{x}{c} \tag{2}$$

Where, t_e represents the thickness of the Coanda trailing edge, and t_F represent the airfoil thickness. c is the chord length. In this study, the settings are: $c = 1m$.

Substituting equation (1) into equation (2) gives the expression for the airfoil thickness that incorporates the Coanda trailing edge thickness.

2.3. Rational Function Fitting

The concept of momentum coefficient (C_μ) is the ratio of the momentum flux of the ejected jet to the momentum flux of the freestream. This ratio is used to measure and control the intensity of the jet expulsion and is an important parameter in the study of circulation control [10]. Its expression is:

$$C_\mu = \frac{\dot{m}U_j}{q_\infty S} = \frac{\rho_j {U_j}^2 A_j}{\frac{1}{2}\rho_\infty v_\infty^2 S} = \frac{2{U_j}^2 h}{v_\infty^2 c} \tag{3}$$

$$U_j = \sqrt{\frac{C_\mu v_\infty^2 c}{2h}} \tag{4}$$

Where, $\dot{m}$ is the mass flow rate of the jet, U_j is the velocity of the jet, q_∞ is the dynamic pressure of the freestream per unit area, S is the reference area of the wing model, ρ_j, U_j and $A_j$are the density, velocity, and jet nozzle area of the jet, respectively, and ρ_∞ and v_∞ are the density and velocity of the freestream, respectively. Taking the C_μ of the jet as input, the boundary conditions at the nozzle are set as a constant temperature static pressure velocity inlet.

This paper introduces a power consumption coefficient for the jet. The power consumption coefficient is the ratio of the energy consumed by the jet to the energy of the incoming flow. Its expression is:

$$C_E = \frac{\int \frac{1}{2}\rho_j {U_j}^3 dA_j}{q_\infty v_\infty S} = \frac{h}{c}\left(\frac{U_j}{v_\infty}\right)^3 \tag{5}$$

$$K_E = \frac{C_l}{C_d + C_E} \tag{6}$$

By introducing the power consumption coefficient obtained from equation (5) into the drag term of the lift-to-drag ratio (K), the equivalent lift-to-drag ratio (K_E) formula (6) is obtained. The K_E can be used to comprehensively assess the aerodynamic benefits and energy consumption.

3. Airfoil Parameter Sensitivity Analysis

The basic airfoil is selected with a thickness of $t = 0.12c$ and a camber of $w = 0$. The Coanda surface is selected with a baseline of $h/c = 0.1\%$, $a/c = 0.013$, and $b/a = 1$. When studying a particular variable, only that variable is varied. The calculation condition is selected as a Mach number $Ma = 0.15$, a Reynolds number $Re = 3 \times 10^6$, and an angle of attack of 0°. Keep the gas ejection velocity at the nozzle constant at $v_{jet} = 115.36\text{m/s}$.

3.1. Circulation Design Parameter Sensitivity Analysis

3.1.1. Nozzle Height

The nozzle heights h/c are 0.02%, 0.06%, 0.1%, and 0.14%. The jet C_μ varies directly with the nozzle height. Figure 3 presents the impact of different nozzle heights. From the characteristics of lift C_L, pitch moment C_m, K, and K_E, it can be observed that as the nozzle height increases, they follow a similar trend. All showing an initial increase followed by a decrease, indicating the existence of a maximum value. The drag coefficient C_D consistently increases with the increase in nozzle height, and the rate of increase slows down after the C_L reaches its maximum value. This indicates that when the nozzle height is small, increasing the nozzle height can significantly enhance the aerodynamic effects produced by the jet. However, beyond the optimal aerodynamic efficiency value, further increasing the nozzle height leads to a deterioration in the aerodynamic characteristics of the model.

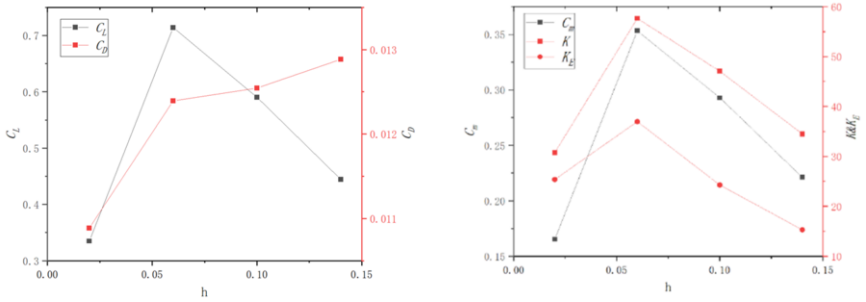

(a) Lift and drag coefficient **(b)** Moment coefficient and lift drag ratio

Figure 3. Effect of jet nozzle height on aerodynamic characteristics.

3.1.2. Radius of Coanda Surface

The model only varies the size of the Coanda surface radius a/c with values of 0.1%, 0.4%, 0.7%, 1.0%, 1.3%, 1.6%, 1.9%, 2.2%, and 2.5%. Figure 4 illustrates the effects of varying Coanda surface radii on aerodynamics. The C_L, C_m, K and K_E show both linear and non-linear increases with radius. At $a/c = 0.001$, lift is near zero, suggesting poor performance. Below this, coefficients rise slowly. Between $0.001 < a/c < 0.016$, they grow rapidly linearly. Above $a/c > 0.016$, lift stabilizes, while drag increases unpredictably. Models in the linear growth phase offer better aerodynamics, and further radius increases post $a/c > 0.016$ provide diminishing returns.

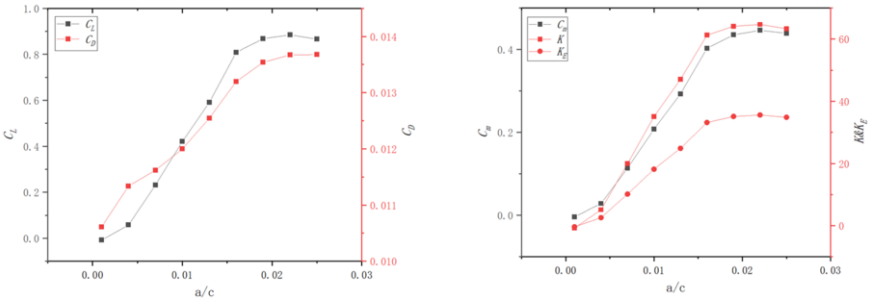

(a) Lift and drag coefficient **(b)** Moment coefficient and lift drag ratio

Figure 4. Effect of the radius of Coanda surface on aerodynamic characteristics.

Fig. 5 shows the velocity distribution at the airfoil's trailing edge for various Coanda surface radii. If the ratio a/c is too small, excessive centripetal force is needed for air deflection, causing the jet to retain its initial direction. It results in a large stagnation area at the lower nozzle that fails to enhance lift effectively. As a/c increases, the attachment angle on the Coanda surface and the aerodynamic benefits improve, with the stagnation point moving closer to the surface. Beyond $a/c = 0.016$, the attachment angle plateaus, the stagnation area enlarges, and the stagnation point moves away, increasing airflow instability and reducing lift. This aligns with literature [11], indicating that larger deflection angles can improve aerodynamics. Therefore, there is an optimal value for aerodynamic benefits, and they do not continue to increase with the increase of the Coanda surface radius.

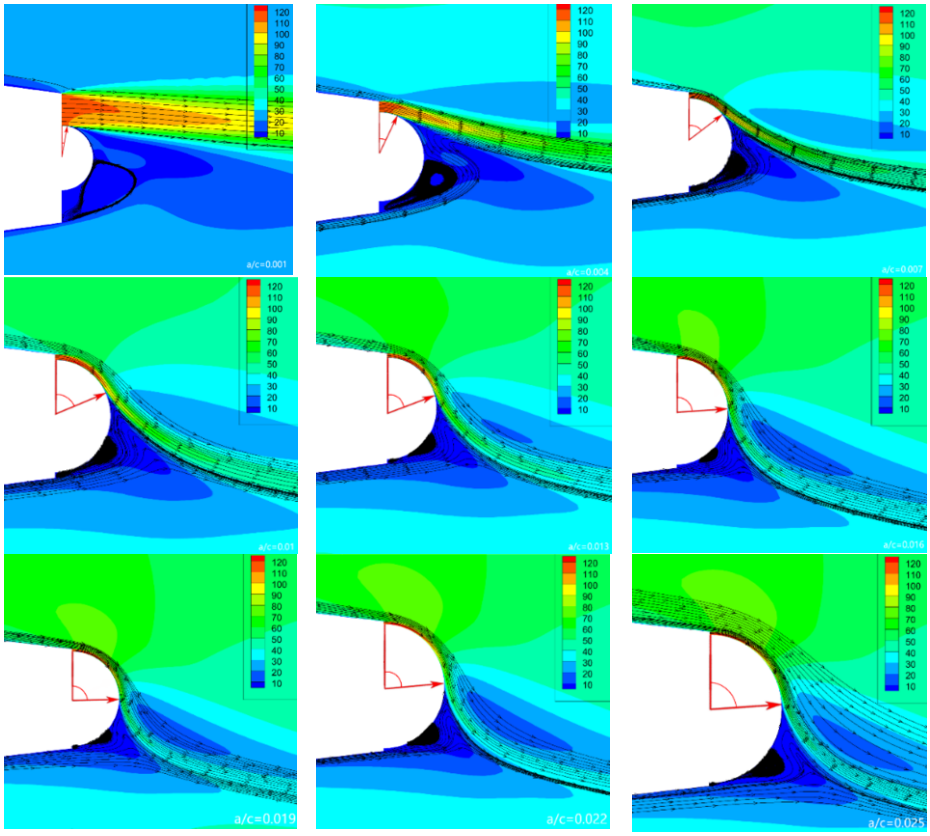

Figure 5. Velocity distribution of trailing edge flow field under different Coanda radius.

3.1.3. Shape of Coanda Surface

The vertical axis height a of the elliptical surface is kept constant, and the horizontal axis height b is varied. The ratio b/a is used to represent the size of the horizontal axis length, with selected values of $b/a = 1/3$、$1/2$、$2/3$、1、$3/2$、2、3. Figure 6 presents the aerodynamic characteristics of models with different shapes of Coanda surfaces under circulation control. If the horizontal axis is less than the vertical axis, i.e., $b/a < 1$, as b/a decreases, the lift and moment characteristics decrease. The C_D first slightly changes and then significantly increases, resulting in a significant decrease in the K and K_E. If

$b/a > 1$, as b/a increases, the C_L and C_m first increase and then decrease, reaching their maximum values around $b/a = 3/2$. The C_D first slightly changes and then significantly decreases, resulting in the K and K_E first increasing and then decreasing. Therefore, when only changing the ratio of the horizontal to vertical axes of the Coanda surface, the C_L, C_m, and K and K_E have optimal values. The C_D always decreases with the increase of the horizontal to vertical ratio. Therefore, as the ratio increases, the aerodynamic characteristics first strengthening and then weakening.

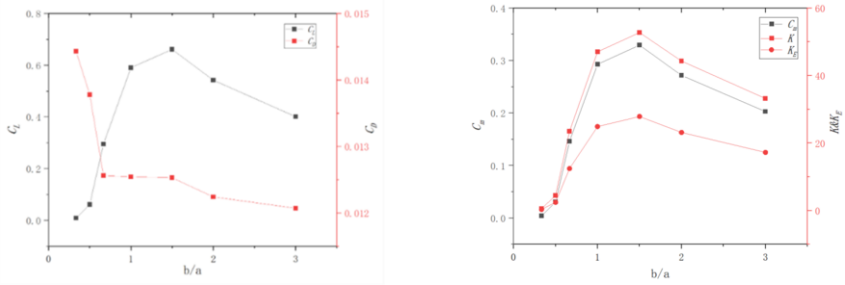

(a) Lift and drag coefficient **(b)** Moment coefficient and lift drag ratio

Figure 6. Effect of the shape of Coanda surface on aerodynamic characteristics.

3.2. Foundation Airfoil Parameter Sensitivity Analysis

To observe the aerodynamic changes of different airfoils as the flow coefficient increases, the aerodynamic characteristics of each model at $C_\mu = 0.005,\ 0.0075,\ 0.01,\ 0.0125,\ 0.015, 0.0175, 0.02$, are studied separately.

3.2.1. Airfoil Thickness

The airfoil thickness t/c is set to 9%, 12%, 15%, 18%, 21%, 24%, and 27% respectively. Figure 7 presents the aerodynamic characteristics of models with different thicknesses as the C_μ varies.

At $C_\mu = 0.005$, the C_L increases significantly with thickness, except for a minor increase when t/c is between 9% and 12%. The C_L consistently show an increasing trend with C_μ, aligning with three distinct regions as the C_μ increases: the linear separated control region (R1), the nonlinear transition region (RT), and the linear super circulation control region (R2) [12]. At t/c of 9% and 12%, the aerodynamics are always in the linear R1 phase within the range of this study's C_μ. At $t/c = 15\%$, the aerodynamic characteristics clearly enter a nonlinear RT phase. As airfoil thickness continues to increase, the RT advances, leading to the emergence of a linear R2, noticeable by $t/c = 27\%$ at $C_\mu = 0.0075$. The rate of increase of the C_L in the R1 phase is better than that in the R2 phase. The C_D increases with both thickness and C_μ, growing slowest in the R1, fastest in the RT, and moderately in the R2. The optimal drag characteristics occur at t/c of 9% to 12%, with rapid increases at greater thicknesses.

In flapless aircraft control, higher C_μ mirror greater deflection of conventional control surfaces [13]. Figure 7(c) shows C_m curves reflecting control effectiveness, where higher C_m values and steeper curve growth indicate better performance. At $t/c = 9\%$ and 12%, growth is steady but low. At $t/c = 15\%$, growth peaks, then slows in the R2 phase. Above $t/c = 15\%$, initial R1 growth is high, but the model's performance declines as it enters the R2 area.

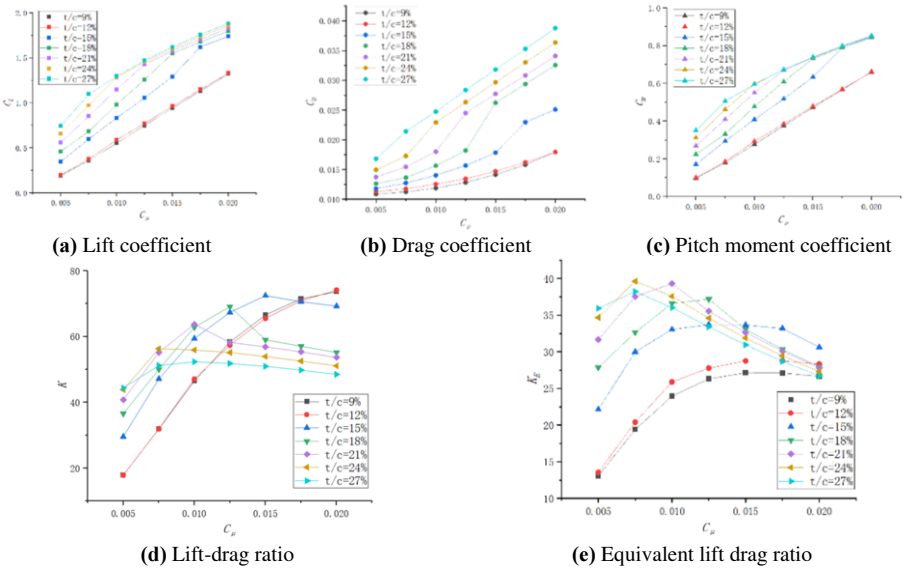

(a) Lift coefficient **(b)** Drag coefficient **(c)** Pitch moment coefficient

(d) Lift-drag ratio **(e)** Equivalent lift drag ratio

Figure 7. Effect of the thickness of airfoil on aerodynamic characteristics.

At $C_\mu = 0.005$, the K peaks at $t/c = 12\%$ surpassing that at $t/c = 9\%$. It slows within $12\% < t/c < 24\%$ and minimally rises at $t/c = 24\%$ and 27%. The K surges in the R1 but plummets in the R2 with increasing C_μ. At $C_\mu = 0.02$, the ratio declines with thickness. Accounting for jet energy consumption, the K_E's gradient drops, clarifying the model's aerodynamic trend. The K_E no longer rising in the R1 and significantly decreasing in the R2. The best one are obtained at $t/c = 15\%$.

3.2.2. Airfoil Camber

The airfoil camber is selected at $w/c = 0\%, 2\%, 4\%, and\ 6\%$ at 0.4 times the chord length. Figure 8 shows the aerodynamic characteristic curves of models with different camber variations as C_μ changes.

Figure 8(a) shows the C_L rising with camber, aligning with theory. At a constant C_μ, C_L growth slows with increasing camber. Aerodynamic characteristics rise with the C_μ. Airfoils at $w/c = 0\%$ maintain a linear lift increase in the separation control zone. Different cambers exhibit similar growth rates in this zone, peaking initially then plateauing. Increasing camber shifts the RT zone earlier. In the R2, C_L growth is slow. Figure 8(b) indicates the C_D rises with both w/c and C_μ, growing fastest in the RT zone and moderately in the R2 zone. Within the separation control region, the wing exhibits the best drag characteristics.

The trend of the C_m is similar to that of the lift characteristics. Considering the aspect of control effectiveness, within the separation control region, the rate of increase in the moment coefficient initially rises with camber augmentation and subsequently declines. Consequently, at zero angle of attack, enhancing camber imparts a notable optimization on the aircraft's control efficiency.

Introducing the jet energy consumption factor clarifies the K trends. At constant C_μ, increasing camber keeps the K_E in positive growth. When $w/c = 0\%$, K_E's growth slows and turns slightly negative as C_μ rises, indicating a late-stage decrease in

separation control. Higher cambers bring forward this negative growth, with $w/c = 4\%$ and 6% showing constant negative K_E trends.

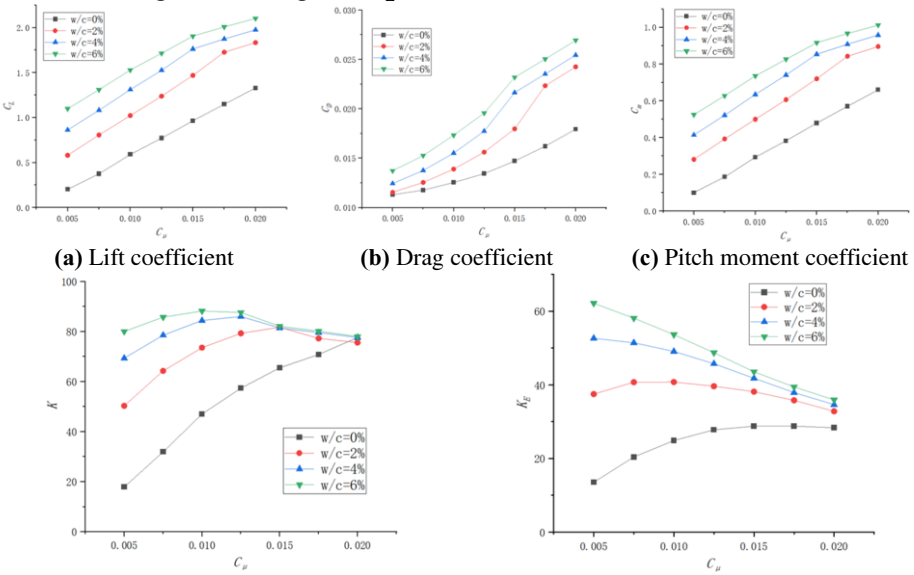

(a) Lift coefficient **(b)** Drag coefficient **(c)** Pitch moment coefficient

(d) Lift-drag ratio **(e)** Equivalent lift drag ratio

Figure 8. Effect of the camber of airfoil on aerodynamic characteristics.

Figures 9 show pressure and velocity distributions for airfoils with varying camber at $C_\mu = 0.01$. As the camber increases, the deflection angle of the jet attached also increases. When $w/c = 6\%$, the jet folds back and deflects in the opposite direction, creating two braking areas before and after the jet. In this case, although the aerodynamic characteristics are good, they are not stable.

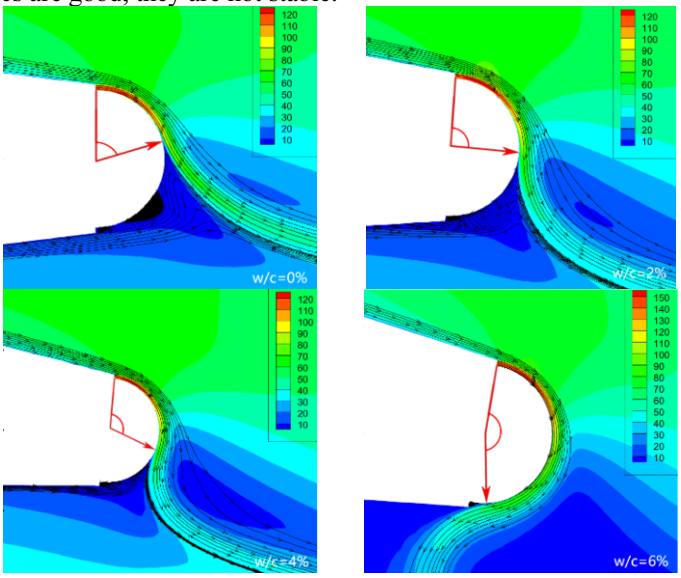

Figure 9. Velocity distribution of trailing edge flow field under different camber.

4. Conclusion

This paper has established an airfoil parametrization model for circulation control airfoils and investigeted the effects of different nozzle heights, radii and shapes of Coanda surface, and airfoil thickness and camber on the circulation control effect. The main conclusions are as follows:

- For nozzle height and Coanda surface shape, the best equivalent lift-to-drag ratio (K_E) are achieved at $h/c = 0.06\%$ and $b/a = 3/2$ respectively. Regarding the Coanda surface radius, K_E cease to change significantly after increasing to $a/c = 0.016$.
- At high momentum coefficients, increasing airfoil thickness not only brings benefits in terms of moment coefficient gains but also significantly reduces the K_E. Considering all factors, the optimal benefits are achieved at $t/c = 15\%$. The same principle applies to airfoil camber, with the best comprehensive benefits achieved at $w/c = 0\%$.

Therefore, the Coanda surface parameters and basic airfoil parameters discussed in this paper both have an impact on aerodynamic benefits. It is necessary to comprehensively consider the aerodynamic benefits obtained, the growth rate, the aerodynamic phase, and energy consumption to select the optimal value for airfoil parameter.

References

[1] ZHANG Y H, ZHANG D C, ZHOU Z W, et al. A review of concept and design of “virtual rudder surface” aircraft based on circulation control[J]. *Acta Aeronautica et Astronautica Sinica*, 2024, 45(6): 629608. doi: 10.7527/S10006893.2023.29608. (in Chinese)

[2] Warsop C. and Crowther W. J. Fluidic Flow Control Effectors for Flight Control [J]. AIAA *JOURNAL*, 2018: 3808-3824. doi: 10.2514/1.J056787.

[3] JONES G S, LIN J C, ALLAN B G, et al. Overview of CFD Validation Experiments for Circulation Control Applications at NASA[C]. International Powered Lift Conference, London, 2008.

[4] ENGLAR R J and HUSON G G. Development of advanced circulation control wing high-lift airfoils[J/OL]. *Journal of Aircraft*, 1984, 21(7): 476-483. doi: 10.2514/3.44996.

[5] Warsop C. and Crowther W. J. Fluidic Flow Control Effectors for Flight Control [J]. AIAA *JOURNAL*, 2018: 3808-3824. doi: 10.2514/1.J056787.

[6] Fielding J. P., Lawson C. P., Pires R., et al. Development of the DEMON Technology Demonstrator UAV [C]. 27TH INTERNATIONAL CONGRESS OF THE AERONAUTICAL SCIENCES, 2010.

[7] Zhao Z J, Luo Z B, Liu J F, et al. Flight test of aircraft three-axis attitude control without rudders based on distributed dual synthetic jets [J]. *Chinese Journal of Theoretical and Applied Mechanics*, 2022, 54(05): 1220-1228. (in Chinese)

[8] Englar R, Jones G, Allan B, et al. 2D circulation control airfoil benchmark experiments intended for CFD code validation [C]// 47th AIAA Aerospace Sciences Meeting Including the New Horizons Forum and Aerospace Exposition. Orlando, USA: AIAA, 2009: 902.

[9] Sobieczky H. Parametric airfoils and wings [J]. *Note on Numerical Fluid Mechanics*, 1998, (68): 71-88.

[10] Jones G S and Joslin R D. Applications of Circulation Control Technology [M/OL]. Reston, VA: American Institute of Aeronautics and Astronautics, 2006. doi: 10.2514/4.866838.

[11] Fu Z J, Chu Y W, Cai Y S, et al. Numerical investigation of circulation control applied to flapless aircraft [J/OL]. *Aircraft Engineering and Aerospace Technology*, 2020, 92(6): 879-893. doi: 10.1108/AEAT-10-2019-0208.

[12] Jones G, Yao C S and Allan B. Experimental investigation of a 2D supercritical circulation-control airfoil using particle image velocimetry [C]// 3rd AIAA Flow Control Conference. San Francisco, California, 2006: 3009-3029.